

# Nonlinear $I$ – $V$ electrical behaviour of doped $\text{CaCu}_3\text{Ti}_4\text{O}_{12}$ ceramics

P. Leret<sup>a,\*</sup>, J.F. Fernandez<sup>a</sup>, J. de Frutos<sup>b</sup>, D. Fernández-Hevia<sup>c</sup>

<sup>a</sup> *Electroceramic Department, Instituto de Cerámica y Vidrio, CSIC, C/Kelsen 5, 28049 Madrid, Spain*

<sup>b</sup> *ETSIT-UPM, Ciudad Universitaria, 28040 Madrid, Spain*

<sup>c</sup> *INAEL, S.A. Pol. Industrial del Jarama s.n., 45007 Toledo, Spain*

Available online 30 March 2007

## Abstract

In this work a comparative study of undoped  $\text{CaCu}_3\text{Ti}_4\text{O}_{12}$  (CCTO) and doped with  $\text{Fe}^{3+}$  (CCTOF) and  $\text{Nb}^{5+}$  (CCTON) ceramics, was aimed to modify the electronic transport. XRD patterns, FE-SEM microstructural analysis, impedance spectroscopy and  $I$ – $V$  response curves were afforded to correlate the microstructure with the nonlinear  $I$ – $V$  behaviour. The appearance of nonlinear behaviour in doped CCTO samples has been correlated with the ceramic microstructure that consists in n-type semiconductor grains, surrounded by a grain boundary phase based on CuO. The presence of this secondary grain boundary phase is the responsible of the assisted liquid phase sintering in CCTO ceramics. Doped samples showed cleaner grain boundaries than CCTO and nonlinearity in the  $I$ – $V$  response.

© 2007 Elsevier Ltd. All rights reserved.

**Keywords:** Grain growth; Grain boundaries; Dielectric properties;  $\text{BaTiO}_3$  and titanates;  $\text{CaCu}_3\text{Ti}_4\text{O}_{12}$

## 1. Introduction

The  $\text{CaCu}_3\text{Ti}_4\text{O}_{12}$  compound, CCTO, has recently attracted much interest due to its extraordinarily high static dielectric constant (up to  $10^5$ )<sup>5</sup> which is practically frequency independent up to  $10^6$  Hz<sup>1</sup> and possesses good temperature stability over a temperature range between  $-173$  and  $127$  °C. This extremely high dielectric constant is usually associated to ferroelectric or relaxor materials. However, CCTO structure remains centrosymmetric at all temperatures with no phase transitions. The unit cell of this titanate was identified in 1979<sup>2</sup> as a body-centred cubic perovskite-like structure with  $Im\bar{3}$  space group and a lattice parameter of  $7.391$  Å. The  $\text{TiO}_6$  octahedra are tilted resulting in the doubling of the perovskite-like lattice parameter, and involving a square planar arrangement of the oxygen around the  $\text{Cu}^{2+}$  cations.<sup>3</sup>

The origin of the giant dielectric constant of CCTO is not fully understood. It is still questionable whether the high dielectric constant is intrinsic to a perfect crystal or extrinsic and related to the material microstructure,<sup>4</sup> as indicated in the grain boundary barrier layer capacitance,<sup>3</sup> IBLC, model. In this model the conductivity of the sample is prevented to percolate by the presence of insulating blocking layers

at the surfaces or at internal domains boundaries. Thus, the behaviour of CCTO can be explained in terms of semi conducting grains and insulating grain boundaries but the presence of a secondary phase at the grain boundary was not previously observed.

Through a combination of micro contact  $I$ – $V$  measurements, Kelvin probe force microscopy, and resistivity and thermoelectric power measurements on individual grains, as well as across grain boundaries, it has been determined that the grains are conducting and are n-type, and a large potential barrier exists at the grain boundaries reflecting their insulating character.<sup>4</sup> Oxygen vacancies may be proposed as a possible cause for the electron formation.<sup>5</sup> In addition to the high permittivity,  $\text{CaCu}_3\text{Ti}_4\text{O}_{12}$  has remarkably nonlinear current–voltage characteristics.<sup>6</sup> An intrinsic electrostatic barrier at the grain boundaries is attributed to be responsible for the nonlinear behaviour. Under dc bias, the grain boundary resistance decreases and the nonlinear response appears with a barrier height estimated to be  $0.82$  eV.<sup>7</sup> The effect of further annealing at different temperatures in oxygen-rich atmospheres allows<sup>8</sup> to conclude that nonohmic electrical properties are originated from a Schottky-type potential barrier, according to a chemical model in which oxygen plays a key role.<sup>8</sup> However, the p-type grain boundary conductivity<sup>8</sup> is attributed to the fact that segregated transition metal oxides are metal deficient and become oxygen enriched. At the same time no secondary grain boundary phases were detected.

\* Corresponding author. Tel.: +34 917355840; fax: +34 917355843.  
E-mail address: [pleret@icv.csic.es](mailto:pleret@icv.csic.es) (P. Leret).

The purpose of the present work is to investigate the effect of acceptor doping,  $\text{Fe}^{3+}$ , and donor doping,  $\text{Nb}^{5+}$ , on the current–voltage behaviour of CCTO material.

## 2. Experimental procedure

Ceramic samples of  $\text{Ca}_{0.25}\text{Cu}_{0.75}\text{TiO}_3$  (CCTO),  $\text{Ca}_{0.25}\text{Cu}_{0.75}\text{Ti}_{0.99}\text{Fe}_{0.01}\text{O}_{2.995}$  (CCTOF) and  $\text{Ca}_{0.25}\text{Cu}_{0.75}\text{Ti}_{0.99}\text{Nb}_{0.01}\text{O}_{3.005}$  (CCTON) were prepared by a conventional solid state reaction and sintering process. The analytical grade  $\text{CaCO}_3$  (Aldrich),  $\text{TiO}_2$  (Merck),  $\text{CuO}$  (Aldrich),  $\text{Nb}_2\text{O}_5$  (Fluka) and  $\text{Fe}_2\text{O}_3$  (Aldrich) powders were mixed for 2 h, by attrition milling with 1.2 mm Zirconia balls using de-ionized water as liquid medium and 0.2 wt% of Dolapix C64 as dispersant. The milled powders were dried and sieved through a 100  $\mu\text{m}$  mesh. The powders were calcined at 900 °C for 12 h and then attrition milled again for 3 h. The organic binders, 0.6 wt% of Polyvinyl alcohol, PVA, and 0.3 wt% of polyethylene glycol, PEG, were added into the calcined powders upon milling to help the formation of compacts. Powders were dried and sieved through a 63  $\mu\text{m}$  mesh and uniaxially pressed at 200 MPa into discs of 8 mm in diameter and 1.3 mm in thickness. Different sintering temperatures were studied to improve the ceramic density and, finally, 1100 °C heating rate 3 °C/min was chosen as it gave the best results. The pellets were sintered in air at 1100 °C for 2, 16 and 32 h and one set was furnace cooled to room temperature, with a cooling rate of 3 °C/min, while the other one was air-quenched on a brass block.

The X-ray diffraction analysis was performed on a Siemens Kristalloflex diffractometer using  $\text{Cu K}\alpha_1$  radiation and Ni filter. Samples were polished and thermally etched at 900 °C during 5 min. The microstructure of the samples was observed by using a Hitachi S-4700 field emission scanning electron microscope, FE-SEM, coupled with energy dispersed spectroscopy, EDS. Polished discs were electroded with room temperature silver paste to form a parallel plate capacitor. The current–voltage ( $I$ – $V$ ) characteristics of the samples were studied using a Keithley 2410 Source meter.

## 3. Results and discussion

The density value of the different sintered samples, ranged from 4.8 to 4.9  $\text{g}/\text{cm}^3$ , and it was similar to the data reported by other authors.<sup>9</sup> Fig. 1 illustrates characteristic XRD patterns of CCTO, CCTOF and CCTON samples sintered for 16 h. The XRD analysis of the undoped and doped CCTO samples showed, also in agreement with previous works, a single perovskite phase. However, high intensity XRD studies on undoped CCTO served to find out traces of a second phase identified as  $\text{CuO}$  (Fig. 2). The presence of secondary phases was previously only found in non-stoichiometric compositions as  $\text{CaTiO}_3$ ,  $\text{CuO}$  and  $\text{Cu}_2\text{O}$ .<sup>9</sup> According to the phase diagram,<sup>10</sup>  $\text{Cu}^{2+}$  cations are reduced at temperatures >1000 °C forming a liquid phase at 1075 °C. During cooling,  $\text{Cu}^{1+}$  is reoxidized as can be confirmed by the presence of the  $\text{CuO}$  phase.

Fig. 3 shows the microstructural evolution of undoped ceramics. Two hour sintered CCTO sample, revealed the presence of a bimodal microstructure composed by exaggerated grain

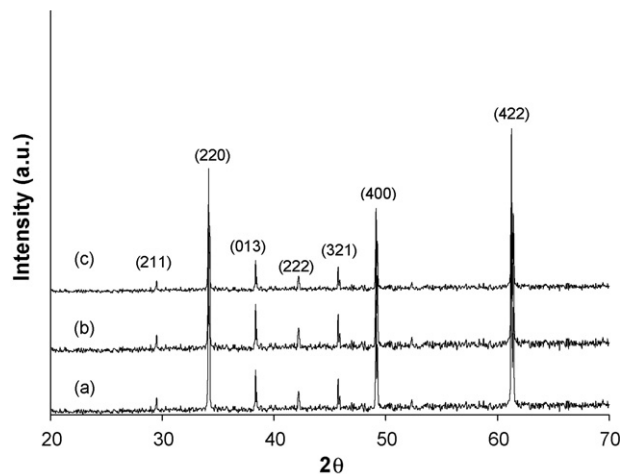


Fig. 1. XRD of (a) CCTO (b) CCTOF and (c) CCTON sintered for 16 h and furnace cooled.

growth grains, >150  $\mu\text{m}$ , having trapped porosity, small grain regions, ~4–6  $\mu\text{m}$ , and a secondary phase that crystallized on the surface and which was, in contrast, more brilliant than the CCTO matrix. This brilliant phase, identified as  $\text{CuO}$ , was analyzed by using EDS as copper oxide and contains ~4 mol% of  $\text{TiO}_2$  in solid solution. In the CCTO 16 h sintering sample, both grain growth and microstructure was uniform, showing large grains with trapped porosity and a secondary phase, generally located at the grain boundaries. The CCTO 32 h sample, showed a decrease in the presence of grain boundary secondary phase and, as a result, cleaner grain boundaries. Liquid-sintering phase, based on a  $\text{CuO}$  phase, seems to be the driven force for the undoped CCTO ceramics and the responsible of the exaggerated grain growth. The presence of  $\text{CuO}$  implies that the solid solution was uncompleted at this stage. As the system reached the equilibrium, the  $\text{CuO}$ -based grain boundary phase was incorporated to the grain. The solubility of Ti-cations in  $\text{CuO}$  and the low surface/volume ratio of grains, allow the presence of  $\text{CuO}$ -based grain boundary phase. This secondary phase recrystallized during the etching thermal treatment at 900 °C, which is a temperature below the liquid appearance. The presence of this kind of grain boundary secondary phase could be on the origin of the

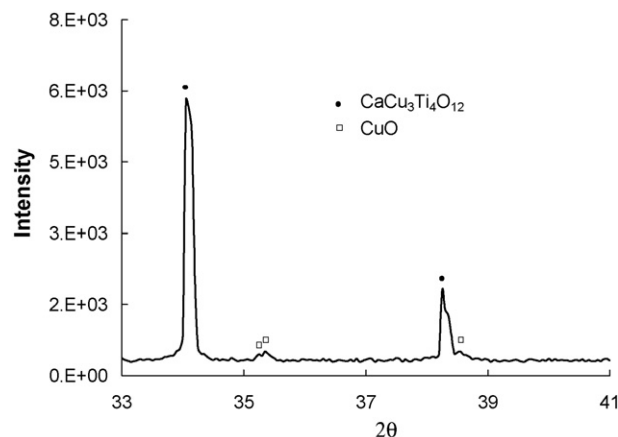


Fig. 2. High intensity XRD of sintered CCTO 16 h and furnace cooled.

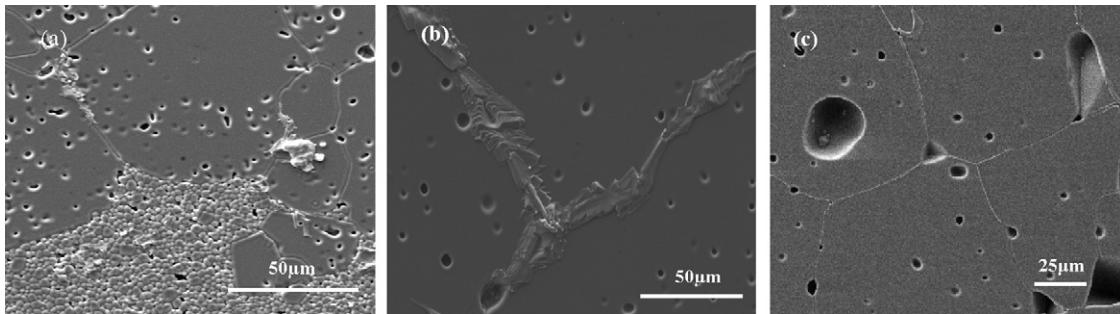


Fig. 3. SEM micrographs of CCTO sintered for (a) 2 h (b) 16 h and (c) 32 h, furnace cooled.

discrepancies between different dielectric values found in the literature.

Both dopants produced grain growth control that was more effective for donor-doped samples at lower sintering time (Fig. 4). The 32 h sintered CCTOF and CCTON microstructures, revealed a grain size  $<50\ \mu\text{m}$  having less grain trapped porosity and an important presence of clean grain boundaries. When the grain boundary phase was evident, its thickness was lower than the observed in CCTO samples.

In contrast to the data published by Chung et al.,<sup>6</sup> both the furnace cooled and quenched undoped CCTO ceramics showed ohmic behaviour in  $I$ – $V$  response (Fig. 5). It was observed that near to the current upper limit of the electrometer some nonlinearities could be interpreted as nonlinear current–voltage behaviour, but uncertainty and lack of reproducibility of these measurements were questioned. Resistivity decreases gradually

as increasing sintering time and the quenched ceramic possesses a remarkable high resistivity.<sup>11</sup>

CuO-based ceramic is confirmed to be a metal deficient p-type semiconductor with copper vacancies generated at low temperature.<sup>12</sup> Undoped CuO ceramic showed a dc resistivity of  $\sim 5\ \Omega\text{cm}$ .<sup>13</sup> When sintering CuO at temperatures higher than  $1000\ ^\circ\text{C}$ , the coexisting  $\text{Cu}_2\text{O}$ , on  $3\ ^\circ\text{C}/\text{min}$  furnace cooled samples increased the resistivity more than an order of magnitude.<sup>12</sup> So, quenched samples could have a higher proportion of reduced phase and thus, grain resistivity increases and controls the overall samples resistivity. The p-type semiconductor nature of grain boundaries, reported by Marques et al.,<sup>8</sup> in sintered samples thermally treated at different oxygen-rich atmospheres, could be correlated with the existence of a second grain boundary CuO-based phase and thus with the nonohmic response appearance.

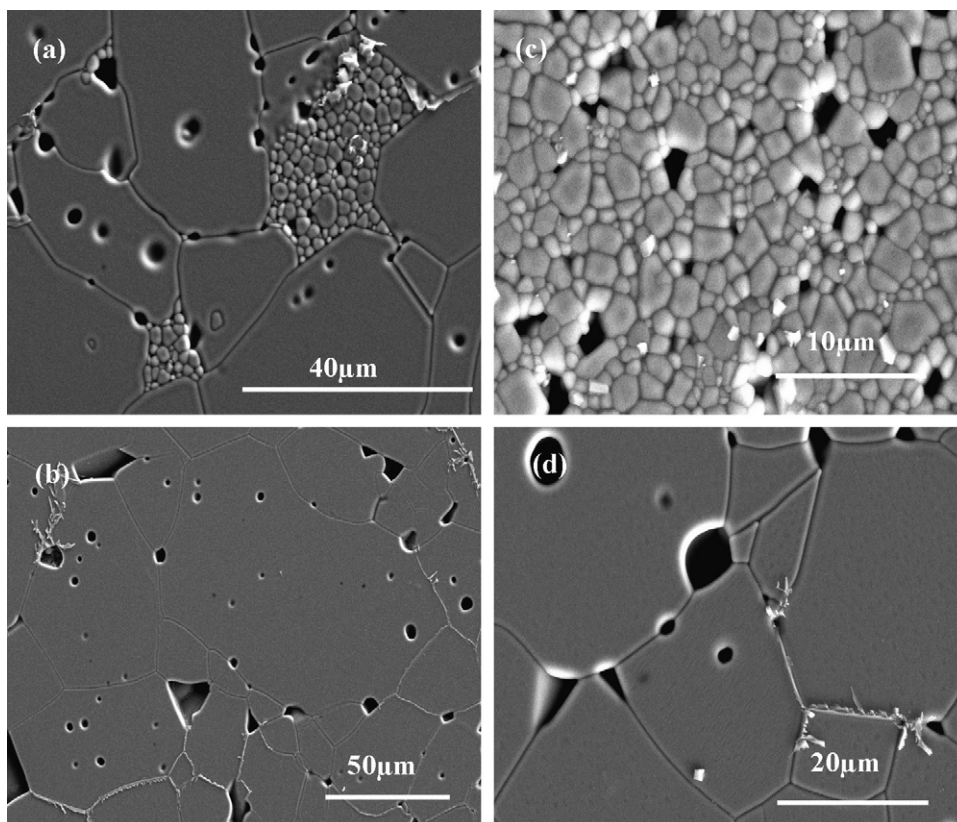


Fig. 4. SEM micrographs of CCTOF sintered for (a) 2 h (b) 32 h and CCTON samples sintered for (c) 2 h and (d) 32 h. All of them furnace cooled.

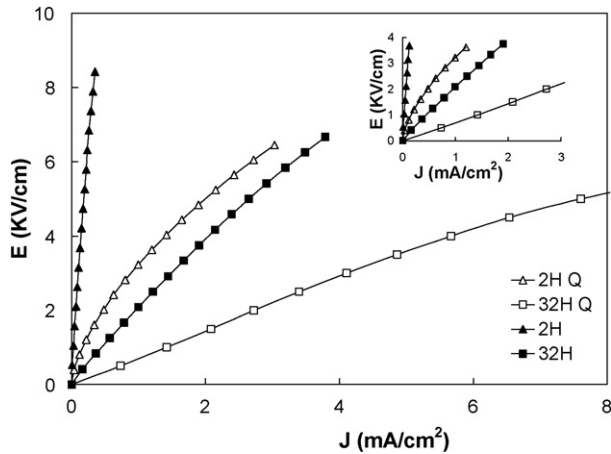


Fig. 5.  $I$ - $V$  behaviour of CCTO samples, sintered for 2 h (triangles) and 32 h (squares). Furnace cooled to room temperature (black symbols) and air-quenched (open symbols).

On the other hand, doped samples, CCTOF and CCTON, showed nonlinear current–voltage characteristics, as shown in Figs. 6 and 7, and the  $I$ - $V$  curves were quite reproducible. In both cases, the breakdown voltage and the resistivity of the linear part of the curve, decrease with increasing the sintering time and in the air-quenched samples. By comparison with undoped CCTO, doped ceramic show lower breakdown voltages even the grain size is quite lower. The nonlinear behaviour of doped samples could be associated with the fact that CCTOF and CCTON have smaller grains than CCTO and CuO secondary phase at the grain boundaries is thinner and it is more spread out. The thinner and the more homogeneous the secondary phase is shared amongst the grain boundaries, the better the rectification of the  $I$ - $V$  curve is. In contrast, CCTO samples possess a very thick grain boundary secondary phase, creating an insulator effect responsible of the material linear behaviour.

The dopants used, favour the incorporation of CuO-based phase into the CCTO structure. To establish a possible similarity with ZnO-based varistors,<sup>14</sup> relating the presence of a

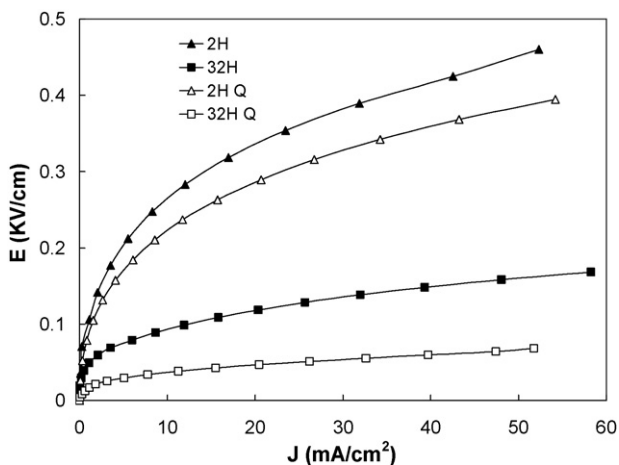


Fig. 6.  $I$ - $V$  behaviour of CCTOF samples sintered for 2 h (triangles) and 32 h (squares). Furnace cooled to room temperature (black symbols) and air-quenched (open symbols).

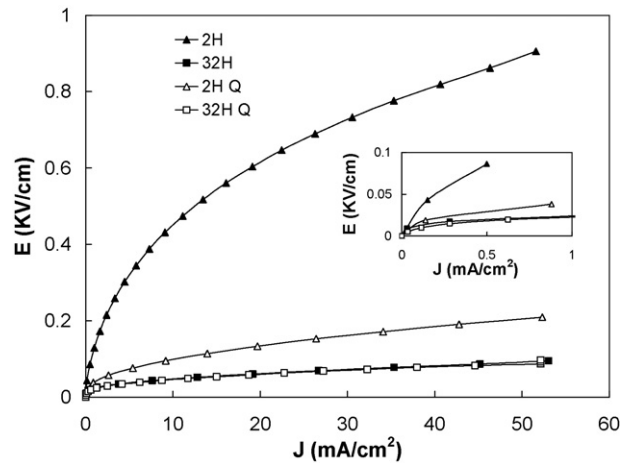


Fig. 7.  $I$ - $V$  behaviour of CCTON samples sintered for 2 h (triangles) and 32 h (squares). Furnace cooled to room temperature (black symbols) and air-quenched (open symbols).

very thin layer of amorphous secondary phase as the origin of high nonlinear properties, would require a more careful TEM observation experiments. Taking into account the reported barrier height<sup>7</sup> (estimated to be 0.82 eV) and the grain size of the sintered CCTON 32 h sample, the breakdown voltage must be 17 V, in good agreement with the observed in Fig. 7. In doped samples the dc resistivity in the nonohmic region, was lower for the quenched samples than for the furnace cooled ones that revealed again the higher grain conductivity.

In addition, the adequate amount and nature of the donor dopant required to maximize grain conductivity<sup>15</sup> and the ceramic processing to control the grain boundary phase nature,<sup>8</sup> would require further studies to optimize nonlinear behaviour in order to facilitate device development.

#### 4. Conclusions

The appearance of nonlinear behaviour in doped CCTO samples has been correlated with the ceramic microstructure which consisted in n-type semiconductor grains surrounded by a grain boundary phase, based on CuO. The presence of a grain boundary CuO-based phase was revealed in undoped CCTO samples and favours the liquid phase sintering of these ceramics. The secondary phase evolved to disappear when increasing the sintering time. Dopants modified the sintering kinetic and produced a limited grain growth control. Doped samples showed cleaner grain boundaries with a very thin secondary phase coat on them, responsible for the nonlinear  $I$ - $V$  behaviour. On the other hand, CCTO's secondary phase is thicker creating an insulator grain boundary and, consequently, a linear behaviour of the  $I$ - $V$  curve.

#### Acknowledgement

The authors express their thanks to the CICYT (Project MAT2004-04843-C02-01) for their financial support.

## References

1. Fang, L., Shen, M., Yang, J. and Li, Z., The effect of SiO<sub>2</sub> barrier layer on the dielectric properties of CaCu<sub>3</sub>Ti<sub>4</sub>O<sub>12</sub> films. *J. Phys.*, 2005, **38**, 4236–4240.
2. Bochu, B., Deschizeaux, M. N. and Joubert, J. C., Synthèse et caractérisation d'une série de titanates perovskites isotopes de CaCu<sub>3</sub>Mn<sub>4</sub>O<sub>12</sub>. *J. Solid State Chem.*, 1979, **29**, 291–298.
3. Brizé, V., Gruener, G., Wolfman, J., Fatyeyeva, K., Tabellout, M., Gervais, M. et al., Grain size effects on the dielectric constant of CaCu<sub>3</sub>Ti<sub>4</sub>O<sub>12</sub>. *Mater. Sci. Eng. B*, 2006, **129**, 135–138.
4. Grubbs, R. K., Venturini, E. L., Clem, P. G., Richardson, J. J., Tuttle, B. A. and Samara, G. A., Dielectric and magnetic properties of Fe- and Nb-doped CaCu<sub>3</sub>Ti<sub>4</sub>O<sub>12</sub>. *Phys. Rev. B*, 2005, **72**, 104111.
5. Sinclair, D. C., Adams, T. B., Morrison, F. D. and West, A. R., One step internal barrier layer capacitor. *Appl. Phys. Lett.*, 2002, **80**(12), 2153–2155.
6. Chung, S. Y., Kim, I. D. and Kang, S. J. L., Strong nonlinear current-voltage behaviour in perovskite-derivative calcium copper titanate. *Nat. Mater.*, 2004, **3**, 774–778.
7. Kim, I. D., Rothschild, A. and Tuller, H. L., Direct current bias affects on the grain boundary Schottky barriers in CaCu<sub>3</sub>Ti<sub>4</sub>O<sub>12</sub>. *Appl. Phys. Lett.*, 2006, **88**, 072902.
8. Marques, V. P., Bueno, P. R., Simoes, A. Z., Cilense, M., Varela, J. A., Longo, E. et al., Nature of potential barrier in (Ca<sub>1/4</sub>Cu<sub>3/4</sub>)TiO<sub>3</sub> polycrystalline perovskite. *Solid State Commun.*, 2006, **138**, 1–44.
9. Guillemet-Fritsch, S., Lebey, T., Boulos, M. and Durand, B., Dielectric properties of CaCu<sub>3</sub>Ti<sub>4</sub>O<sub>12</sub>. *J. Eur. Ceram. Soc.*, 2006, **26**, 1245–1257.
10. Withler, J. D. and Roth, R. S., *Phase Diagrams for high Tc Superconductors, Compiled in the phase diagrams for Ceramists Data Centre*. National Institute of Standards and Technology, Ohio, 1991, p. 1.
11. Shao, S. F., Zhang, J. L., Zheng, P., Zhong, W. L. and Wang, C. L., Microstructure and electrical properties of CaCu<sub>3</sub>Ti<sub>4</sub>O<sub>12</sub> ceramics. *J. Appl. Phys.*, 2006, **99**, 08410610.
12. Jeong, Y. K. and Choi, G. M., Nonstoichiometry and electrical conduction of CuO. *J. Phys. Chem. Solids*, 1995, **57**(1), 81–84.
13. Tanaka, S., Sawai, Y. and Chiba, A., Electrical properties and microstructure of CuO ceramics containing small amounts of alkaline earth elements. *J. Eur. Ceram. Soc.*, 2004, **24**, 289–293.
14. Peiteado, M., Zinc oxide-based ceramic varistors. *Bol. Soc. Esp. Ceram. V*, 2005, **44**, 77–87.
15. Brzozowski, E., Caballero, A. C., Villegas, M., Castro, M. S. and Fernandez, J. F., Effect of doping method on microstructural and defect profile of Sb-BaTiO<sub>3</sub>. *J. Eur. Ceram. Soc.*, 2006, **26**, 2327–2336.